

Stability and Transient Dynamics of PLLs in Theory and Experiments

Rabia Fatima Riaz^{*§}, Dimitrios Prousalis[†], Christian Hoyer^{*}, Jens Wagner^{*‡},
Frank Ellinger^{*‡}, Frank Jülicher[†] and Lucas Wetzel[†]

^{*}Chair for Circuit Design and Network Theory, Technische Universität Dresden, Germany

[†]Max Planck Institute for the Physics of Complex Systems, Dresden, Germany

[‡]Centre for Tactile Internet with Human-in-the-Loop (CeTI), Technische Universität Dresden, Germany

[§]rabia_fatima.riaz@tu-dresden.de

Abstract—This paper presents a generalization of the classical phase-locked loop (PLL) theory. It includes the effects of time-delays and mutual coupling between PLLs. Two methods for finding stable solutions to locked states and their transient dynamics are discussed. The theoretical predictions of these methods are verified by experimental measurements obtained of a classical PLL entrained by a clock. For entrainment the generalized and classical PLL theory overlap. The analysis correctly predicts the phase-relations of phase-locked states, the loop-gain dependency on the component characteristics and time-delays and the transient dynamics, i.e., perturbation decay rate and the frequency of perturbation decay. Thus the generalized theory allows a deeper understanding of a PLL's response. The model covers PLLs of arbitrary order and number of inputs.

Index Terms—phase locked loops, delays, control theory, clock synchronization, frequency synchronization, synchronous clocking

I. INTRODUCTION

The conventional approach to global synchronous clocking in digital timing systems is to distribute a clock signal in a spatially distributed system through a tree-like network. This is a hierarchical approach to clock synchronization, a central reference oscillator entrains multiple phase-locked loops (PLLs) in the network [1]. In the classical sense a PLL is a negative feedback system in which the phase of the output signal locks to that of a reference clock. The PLL changes from its quiescent frequency to that of the reference signal and a constant phase-relation can be achieved that need not be zero. In applications that rely on specific phase-relations, such as beam steering and local positioning, it is important to know how the phase-relations depend on the systems' parameters. Furthermore, as the physical extent of the network becomes larger, the clocks suffer from skew and signal propagation delays. Approaches that rely on a mutual coupling of PLLs, sometimes termed self-synchronization, have been explored but did not include effects of such time-delays, which strongly affect the dynamics of such systems [1], [2]. Reference [3] includes the effect of these time delays but there is a need to verify the predicted results, i.e., the phase differences, perturbation decay rate and frequency. This paper presents a

This work was supported by the Federal Ministry of Education and Research (BMBF) within the VIP+ validation program 'PLL-Synchronization' (03VP06431).

theoretical approach to PLL theory, which includes the effect of time-delays and allows to calculate phase-differences and frequencies, as well as the stability of entrained and synchronized states, i.e., phase-locked states. Furthermore, the results predicted by the theory are verified by measurements obtained of a classical PLL entrainment. In time and Laplace domain it is shown how the propagation delay affects the properties of locked states and the transient dynamics of the perturbation response. The paper is organized as follows. Section II introduces the time and Laplace domain representation of the phase model that characterizes the PLL. These representations are used in section III to obtain the characteristics of the phase-locked states. A hardware setup, described in section V, is then used to verify the theoretical results from both methods and the measurements are compared with the theoretical predictions in section IV.

II. GENERALIZED PLL THEORY

Here two representations that characterize phase-locked states of a PLL are introduced and a relation between them is established.

A. Generic phase-model for arbitrary PLL networks

In time-domain, a PLL can be represented as shown in Fig. 1a, see [3]. The phase-detector (PD) receives an external signal $x_l(t - \tau)$ with phase $\phi_l(t - \tau)$ delayed by a time τ from, e.g., the reference clock or another PLL. It is processed together with the feedback-signal of voltage controlled oscillator (VCO) whose frequency is divided v -times. The PD output voltage of PLL k is a function of the phase-difference

$$x_k^{\text{PD}}(t) = \frac{\xi}{2} + h \left[\phi_l(t - \tau) - \frac{\phi_k^{\text{VCO}}(t)}{v} + \phi_k^{\text{INV}} \right] + \mathcal{O}(\text{HF}), \quad (1)$$

where $\phi_k^{\text{VCO}}(t)$ the VCO signals' phase and $h(\cdot)$ is the 2π -periodic phase error transfer function. It is a cosine for multiplier PDs with $\xi = 0$ and a triangular function for XOR PDs with $\xi = 1$ [3], [4]. The piece-wise linear triangular function is $-A_k^{\text{PD}} x/\pi - A_k^{\text{PD}}/2$ for $x \in [-\pi, 0]$ and $A_k^{\text{PD}} x/\pi - A_k^{\text{PD}}/2$ for $x \in (0, \pi]$, where A_k^{PD} denotes amplitude (peak to peak) of the PD output signal. The term ϕ_k^{INV} relates to signal inversion (INV) where $\phi_k^{\text{INV}} = \pi$ for an odd number and $\phi_k^{\text{INV}} = 0$ for an even number of inverters. Assuming an

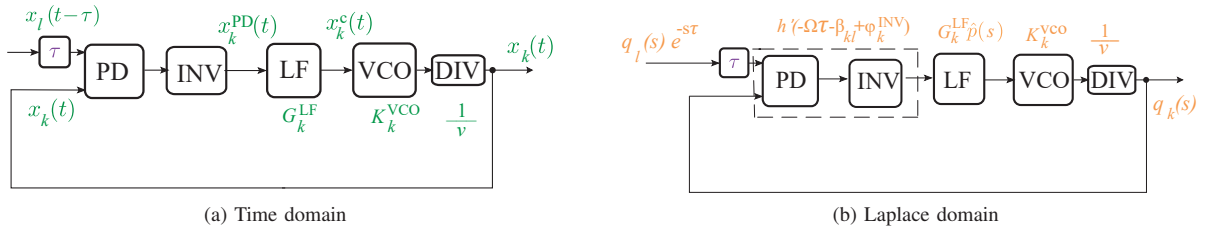


Fig. 1. Time (a) and Laplace domain (b) representation of a phase locked loop.

ideal low pass loop filter (LF) which fully removes the high frequency components $\mathbb{O}(\text{HF})$, the control voltage is

$$x_k^c(t) = G_k^{\text{LF}} \int_0^\infty du p(u) x_k^{\text{PD}}(t-u), \quad (2)$$

where $p(u)$ denotes the impulse response of the LF and G_k^{LF} the loop filter DC gain. This voltage controls the VCO, either increasing or decreasing its instantaneous angular frequency

$$\dot{\phi}_k^{\text{VCO}}(t) = \omega_0 + K_k^{\text{VCO}} x_c(t), \quad (3)$$

where ω_0 is the VCO's quiescent frequency and K_k^{VCO} its sensitivity. Using Eqs. (1-3) and $\dot{\phi}_k(t) = \dot{\phi}_k^{\text{VCO}}(t)/v$ yields

$$\dot{\phi}_k(t) = \frac{\omega}{v} + \frac{K}{v} \sum_{l=0}^N c_{kl} \int_0^\infty du p(u) h[\Delta\phi_{kl}(u, \tau)], \quad (4)$$

where $\Delta\phi_{kl}(u, \tau) = \phi_l(t-u-\tau) - \phi_k(t-u) + \phi_k^{\text{INV}}$ the phase-difference at the PD, c_{kl} equals one if k receives input from l or zero otherwise, $\omega = \omega_0 + \xi G_k^{\text{LF}} K_k^{\text{VCO}}/2$ denotes the intrinsic frequency of the free-running closed-loop PLL and $K = K_k^{\text{VCO}} G_k^{\text{LF}}$ the coupling strength. The global frequency Ω and phase-differences β_{kl} in a phase locked state and its stability can be obtained self-consistently using the approach

$$\phi_k(t) = \Omega t + \beta_k + \epsilon q_k(t), \quad (5)$$

in Eq. (4), where $\epsilon q_k(t)$ is a small phase perturbation [3]. Linearizing about such states the perturbation dynamics are

$$\dot{q}_k(t) = \sum_{l=0}^N c_{kl} \alpha_{kl} \int_0^\infty du p(u) (q_l(t-u-\tau) - q_k(t-u)), \quad (6)$$

where $\alpha_{kl} = K h'(-\Omega\tau - \beta_{kl} + \phi_k^{\text{INV}})/v$ and $h'(\cdot)$ denotes the derivative of the phase error transfer function. This perturbation response can be represented in Laplace domain, see Fig. 1b.

$$s q_k(s) = \sum_{l=0}^N c_{kl} \alpha_{kl} \hat{p}(s) (q_l(s) e^{-\tau s} - q_k(s)). \quad (7)$$

$$\mathcal{L}^{-1} \left[\frac{1}{s} \cdot H_{\text{CL}}(s) \right] = \begin{cases} \text{unstable solution} & \text{if } \zeta < 0, \\ \mathbf{u}(t-\tau) \left\{ 1 - e^{-\zeta \omega_n (t-\tau)} \left[\cos(\omega_d (t-\tau)) + \frac{\zeta}{\sqrt{1-\zeta^2}} \cdot \sin(\omega_d (t-\tau)) \right] \right\} & \text{if } 0 \leq \zeta < 1, \\ \mathbf{u}(t-\tau) \left\{ 1 - e^{-\omega_n (t-\tau)} [1 + \omega_n (t-\tau)] \right\} & \text{if } \zeta = 1, \\ \mathbf{u}(t-\tau) \left\{ 1 - \frac{e^{-[(\zeta - \sqrt{\zeta^2 - 1}) \cdot \omega_n (t-\tau)]}}{2\sqrt{(\zeta^2 - 1)(\zeta - \sqrt{\zeta^2 - 1})}} \right\} & \text{if } \zeta > 1. \end{cases} \quad (11)$$

B. Generic phase-model for the entrainment case

In the case of entrainment of a PLL by a reference clock, i.e., $q_l(s) = q_R(s)$, $\Omega = \omega_R$ and dropping index k , the phase-difference is obtained from Eqs. (4-5)

$$\beta = -\omega_R \tau - h^{-1} \left[\frac{\omega_R v - \omega}{K} \right] + \phi_{\text{INV}}, \quad (8)$$

where $h^{-1}(\cdot)$ denotes the inverse phase error transfer function. It is a multivalued function that leads to multiple solutions, e.g. $\beta = \pm\pi/2$. From Eq. (7) the transfer function can be obtained

$$H_{\text{CL}}(s) = \frac{q(s)}{q_R(s)} = \frac{\alpha \hat{p}(s) e^{-\tau s}}{s + \alpha \hat{p}(s)}. \quad (9)$$

Here, $\alpha = K h'(-\omega_R \tau - \beta + \phi_{\text{INV}})/v$, defines the loop-gain of the PLL which in general depends on the delays and the component heterogeneity, especially in the case of mutually coupled PLLs [3]. However replacing β with the expression in Eq. (8) yields $\alpha = K h'(h^{-1}((\omega_R v - \omega)/K))/v$. Hence, the loop gain is independent of delays for classical PLLs. Using $\hat{p}(s) = (1 + s\tau_c)^{-1}$ for a first order loop filter where τ_c is the time constant of the LF yields

$$H_{\text{CL}}(s) = \frac{\frac{\alpha}{\tau_c} e^{\tau_c s}}{s^2 + \frac{s}{\tau_c} + \frac{\alpha}{\tau_c}}. \quad (10)$$

Comparing Eq. (10) with the transfer function of a second order control system, i.e., $\omega_n^2/(s^2 + 2\zeta\omega_n s + \omega_n^2)$, one identifies for the natural frequency $\omega_n = \sqrt{\alpha/\tau_c}$ and for the damping ratio $\zeta = (2\omega_n \tau_c)^{-1} = (4\tau_c \alpha)^{-1/2}$.

III. STABILITY AND TRANSIENT DYNAMICS

A. Method 1: LTI Systems Control Theory

The stability and transient dynamics of the PLL are given in Eq. (11), derived from Eq. (10) by analyzing the PLL response to a step input change $1/s$ and taking its inverse Laplace transform [5]. Here $\omega_d = \omega_n \sqrt{1 - \zeta^2}$ denotes the frequency of the underdamped perturbation decay case, i.e., $0 \leq \zeta < 1$.

B. Method 2: Linear Stability Analysis

The analysis above becomes difficult for higher orders of loop filters. Therefore a similar method for the linear stability analysis of a PLL, explained in detail in [3], can be used. Assuming an exponential perturbation, i.e., $q(t) = q^0 e^{st}$, where $s = \sigma + i\gamma$ characterizes the dynamic perturbation response. The perturbation response is σ and frequency of perturbation is given by γ . This perturbation is used in Eq. (6), thus obtaining the following characteristic equation

$$s_i + \frac{K \hat{p}(s_i)}{v} h' [-\omega_R \tau - \beta + \phi_{\text{INV}}] = 0. \quad (12)$$

Solving yields a set of solutions $\{s_i\}$ and the system is stable if and only if all $\sigma_i < 0$, i.e., the perturbation decays. Note that the characteristic equation is equal to the denominator of the transfer function.

IV. MEASUREMENTS AND RESULTS

In order to validate the above methods, measurements are taken for the PCB-based PLLs with off-the-shelf components. The PCB and the measurement setup from [6] are modified to characterize the transient response of a PLL with first order loop filter for the entrainment case. Fig. 2 presents the PLL block diagram and Table I lists all its parameters. A fully differential XOR logic gate *MC100EP08* from *ON Semiconductor* is used as a PD whose output is converted to a single-ended signal using an *AD8000* op-amp from *Analog Devices*. This op-amp operates as an adder for the prebias voltage V_{prebias} , inverting the signal in the process. This voltage

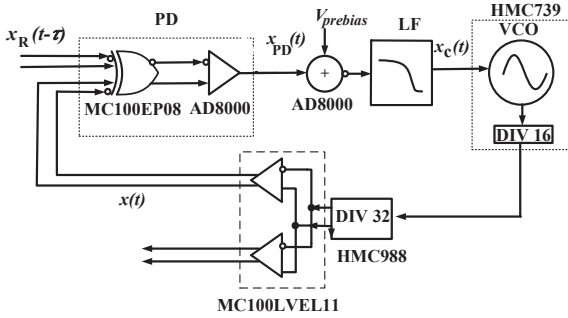


Fig. 2. Block diagram of the PLL composed of off-the-shelf components. Figure modified from Fig. 7 in [6].

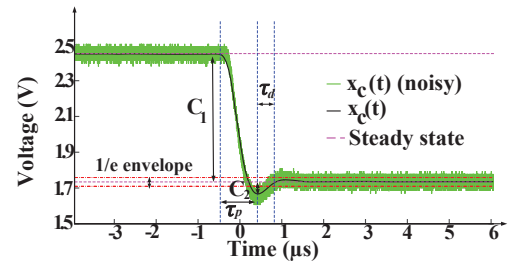
TABLE I
IMPORTANT PARAMETERS OF THE PLL

Description	Parameter	Value
Insertion loss of LF	G_{LF}	1
Cut-off frequency of the first order LF	ω_c^{LF}	$2\pi \cdot 1 \cdot 10^6 \text{ rad}$
Time constant of the first order LF	τ_c	0.159 μsec
Pre-bias Voltage for the VCO	V_{prebias}	2.12 V
Intrinsic frequency of PLL	ω	$2\pi \cdot 24.25 \text{ rad GHz}$
Reference clock frequency	ω_R	$2\pi \cdot 47.36 \text{ rad MHz}$
VCO sensitivity	K_{VCO}	$2\pi \cdot 757 \frac{\text{rad}}{\text{V}} \text{ MHz}$
Division factor of the DIV	v	512
Inverter contribution to the phase	ϕ_{INV}	π
Amplitude of PD output signal	A_{PD}	1.6 V

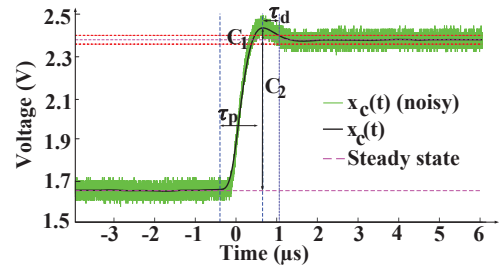
is used to tune the VCO's free-running frequency to 24 GHz. A low pass RC filter suppresses the high frequency components of the PD signal. The resulting control voltage $x_c(t)$ is fed to the *Analog Devices HMC988* VCO, which allows operation in microwave frequency range of 24 GHz. This VCO has a built-in divider of 16, which is used with a separate programmable divider *HMC988*, to yield a total division factor of 512.

V. EXPERIMENTAL SETUP

A reference signal generated by *Keysight 33600A series* signal generator is fed to the PD using *Rosenberger LU1-001-XXX* cables. Here the XXX corresponds to the used cable length. Different propagation delays between 2.64–10.12 ns are obtained by varying the length of the cables between 50–190 cm. The propagation delay of signal in the feedback path is 0.91 ns, so the effective delay of the clock is 1.73–9.21 ns. The PLL is allowed to achieve a steady locked condition (at a reference frequency of 47 MHz) and is then given a step frequency input change by frequency shift keying with a frequency hop of 1 MHz. The response of the PLL to this change is directly captured by the control voltage $x_c(t)$. This signal is observed on a *Rohde & Schwarz RTO-2044* oscilloscope using high impedance (1 M Ω), *RT-ZD40* differential active probes for both the falling edge, i.e., clock's frequency shifts from 48 MHz to 47 MHz, see Fig. 3a and rising edge, i.e., clock's frequency shifts from 47 MHz to 48 MHz, see Fig. 3b. For each case, the noisy data is smoothed in Matlab by applying a Gaussian-weighted moving average filter with window length 10950. Subsequently, PLL parameters can be directly observed and measured through analysis of the waveform according to the following well known equations.



(a) Falling edge



(b) Rising edge

Fig. 3. Transient response of the control voltage $x_c(t)$ for an input frequency change of 1 MHz.

$$\text{Decay rate} = \sigma_{\text{meas}} = -\zeta \omega_n = \frac{1}{\tau_d}, \quad (13)$$

where τ_d is the time constant of the decay, obtained when the overshoot decays to $1/e$ of its peak value in the regime labeled as ‘ $1/e$ envelope’ in Fig. 3.

$$\text{Decay frequency} = \gamma_{\text{meas}} = \omega_d = \frac{\pi}{\tau_p}, \quad (14)$$

where τ_p is the time it takes to reach the minimum or maximum value.

$$\text{Damping ratio} = \zeta = \left(1 + \left[\frac{\pi}{\ln \frac{C_1}{C_2}} \right]^2 \right)^{-\frac{1}{2}}. \quad (15)$$

Both the clock and PLL signal are converted from differential to single-ended signals for each channel of the oscilloscope using *Prodyn Model BIB 100 G* baluns. The clock’s and PLL’s phase is extracted from the signals’ time-series using the Hilbert transform after smoothing them with a moving average. The phase difference is then obtained from the phases of the individual signals.

The results obtained from the measurements are presented in Fig. 4 and compared to theoretical predictions from the two methods discussed in section III. The decay rate and frequency are calculated using the Laplace domain analysis, i.e., $(\frac{2\pi\zeta\omega_n}{\omega_R}, \frac{\omega_d}{\omega_R})$ and the solutions $(\frac{2\pi\sigma}{\omega_R}, \frac{\gamma}{\omega_R})$ obtained from linear stability analysis. The results show good agreement with the measurements $(\frac{2\pi\sigma_{\text{meas}}}{\omega_R}, \frac{\gamma_{\text{meas}}}{\omega_R})$. The analysis also gives an unstable solution with normalized perturbation decay rate of 0.06 for all delays. The theoretical analysis predicts underdamped oscillations, with $\zeta = 0.58$ as compared to $\zeta = 0.60$ obtained from measurements by averaging the results for each delay, see Eq. (15). Fig. 5 compares the phase-relations predicted by model with measurements for the falling and rising edges of the control signal. The decay rate $\sigma = -\zeta \cdot \omega_n = \frac{1}{\tau_c}$ depends only on the loop filter parameters and not explicitly on the delay τ . However, the phase offset is dependent on the delay and is different for the rising and falling edge due to different detuning, i.e., $(w_R v - w)$ when the PLL achieves steady state, see Eq. (8).

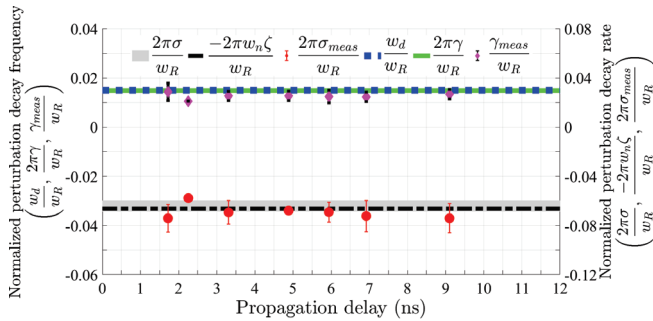


Fig. 4. Decay rates and frequencies obtained from the different methods. All frequencies are normalized by ω_R and all decay rates are normalized by $2\pi/\omega_R$, the period.

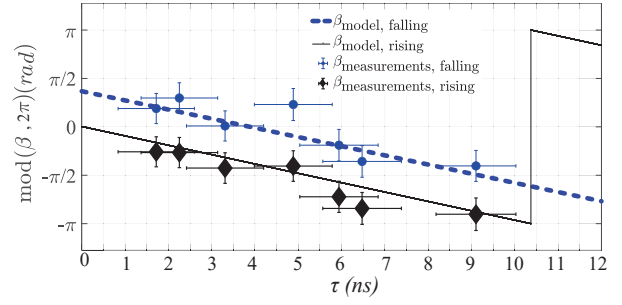


Fig. 5. Phase-difference between clock and PLL for different detuning of the intrinsic frequencies.

VI. CONCLUSION

This work highlights how the classical PLL theory can be understood and extended within the framework of dynamical systems theory. This is verified by experiments in regimes covered by both theories. Furthermore, the extended model unifies the study of hierarchical and self-organized synchronization. It allows to study cases e.g mutual PLL coupling in the presence of time-delays that were out of scope of the classical theory before. The phase model of a PLL is studied in the time and Laplace domain. Its stability and transient dynamics are determined using two methods and the theory is verified by measurements for the case of entrainment. The loop gain is independent of delay for classical PLLs but dependent on delays and component heterogeneity for mutually coupled PLLs. The analysis show that the PLL achieves lock even in the case of significant delays in the case of entrainment. However, the delay contributes to the phase offset between clock and PLL, which can be accurately calculated using the model.

ACKNOWLEDGMENT

We would like to pay our regards to J. Fritzsche and M. Böttcher for inspiring discussions. We acknowledge the cooperation with the Centre for Tactile Internet with Human-in-the-Loop (CeTi), a Cluster of Excellence at TU Dresden, in the area of millimeter-wave circuits.

REFERENCES

- [1] G. A. Pratt and J. Nguyen, “Distributed synchronous clocking,” *IEEE transactions on parallel and distributed systems*, vol. 6, 1995.
- [2] F. M. Orsatti, R. Carareto, and J. R. C. Piqueira, “Mutually connected phase-locked loop networks: dynamical models and design parameters,” *IET Circuits Devices & Systems*, vol. 2, no. 6, pp. 495–508, 2008.
- [3] L. Wetzel, D. J. Jörg, A. Pollakis, W. Rave, G. Fettweis, and F. Jülicher, “Self-organized synchronization of digital phase-locked loops with delayed coupling in theory and experiment,” *PLOS One*, 2017.
- [4] A. Pollakis, L. Wetzel, D. J. Jörg, W. Rave, G. Fettweis, and F. Jülicher, “Synchronization in networks of mutually delay-coupled phase-locked loops,” *New Journal of Physics*, vol. 16, no. 11, p. 113009, 2014.
- [5] Electrical4U. (2019, Oct) Time response of second order control system. [Online]. Available: <https://www.electrical4u.com/time-response-of-second-order-control-system>
- [6] C. Hoyer, D. Prousalis, J. Wagner, R. Riaz, F. Jülicher, L. Wetzel, and F. Ellinger, “Synchronization of Two Delay-Coupled PLL Systems at 24 GHz,” 2020, unpublished.